

# Entanglement dynamics in the three-dimensional Anderson model

Yang Zhao,<sup>1,\*</sup> Dingyi Feng,<sup>1,†</sup> Yongbo Hu,<sup>1</sup> Shutong Guo,<sup>1</sup> and Jesko Sirker<sup>2,3,‡</sup>

<sup>1</sup>*Shanxi Key Laboratory of Condensed Matter Structures and Properties,  
School of Physical Science and Technology, Northwestern Polytechnical University, Xi'an 710072, China*

<sup>2</sup>*Department of Physics and Astronomy, University of Manitoba, Winnipeg R3T 2N2, Canada*

<sup>3</sup>*Manitoba Quantum Institute, University of Manitoba, Winnipeg R3T 2N2, Canada*

(Dated: October 15, 2020)

We numerically study the entanglement dynamics of free fermions on a cubic lattice with potential disorder following a quantum quench. We focus, in particular, on the metal-insulator transition at a critical disorder strength and compare the results to the putative many-body localization (MBL) transition in interacting one-dimensional systems. We find that at the transition point the entanglement entropy grows logarithmically with time  $t$  while the number entropy grows  $\sim \ln \ln t$ . This is exactly the same scaling recently found in the MBL phase of the Heisenberg chain with random magnetic fields suggesting that the MBL phase might be more akin to an extended critical regime with both localized and delocalized states rather than a fully localized phase. We also show that the experimentally easily accessible number entropy can be used to bound the full entanglement entropy of the Anderson model and that the critical properties at the metal-insulator transition obtained from entanglement measures are consistent with those obtained by other probes.

## I. INTRODUCTION

Entanglement measures have been shown to be a useful tool to investigate the non-equilibrium dynamics of quantum systems. Because entangling two previously unentangled regions generally requires the exchange of some entangled entities, they provide direct insights into the quasiparticle dynamics of a many-body system [1]. For a typical clean quantum lattice system with short-range interactions, excitations will spread in a lightcone-like fashion with a finite Lieb-Robinson velocity [2, 3]. This leads to a linear increase of the von-Neumann entanglement entropy  $S$  following a quench from an unentangled initial state and ultimately to a saturation at long times to a value proportional to the volume of the considered region. This behavior is expected to be modified in systems with disorder. The spreading of quasiparticles is then no longer ballistic and the saturation values are reduced as compared to the clean case.

The exact behavior depends on the type and strength of the disorder, the dimensionality of the system, whether or not the system is interacting, as well as other microscopic details such as the range of interactions and the properties of the initial state [4–12]. For one-dimensional non-interacting quantum lattice models with short-range hoppings, any amount of potential disorder is known to lead to the Anderson localization of all eigenstates [13–16]. The saturation values of the entanglement entropy after a quench are then proportional to the localization length. In the two-dimensional case, potential disorder also always leads to the localization of all eigenstates. The entanglement dynamics following a quantum quench

is, however, much more interesting than in the one-dimensional case. Whereas in one dimension an initial sub-ballistic growth of the entanglement entropy is immediately followed by saturation, an extended intermediate time regime does exist in the two-dimensional case for weak disorder. This is due to the fact that in this case the localization length can be much larger than the mean free path. In this regime of weak localization, the entanglement entropy after a quench grows logarithmically in time [11]. Another interesting case which has been studied previously are one-dimensional non-interacting lattice models with off-diagonal (bond) disorder [9, 17]. These systems are driven towards an infinite randomness fixed point characterized by a localization-delocalization transition in the eigenstate energy [18–22]. As a consequence, the entanglement entropy after a quench never saturates but grows in the thermodynamic limit without bounds as  $S \sim \ln \ln t$  [9].

To gain even more insights into quench dynamics based on entanglement probes, one can make use of the fact that for a system with particle number conservation the reduced density matrix  $\rho$ —obtained after tracing out a part of the system—will have a block structure. The von-Neumann entanglement entropy can then be split into two parts [12, 23–35]

$$\begin{aligned} S &= -\text{tr}\{\rho \ln \rho\} \\ &= -\sum_n p(n) \ln p(n) - \sum_n p(n) \text{tr}\{\rho(n) \ln \rho(n)\}. \end{aligned} \quad (1)$$

The first part is the number entropy  $S_N$  and the second part the configurational entropy  $S_{\text{conf}}$ . The probability to find  $n$  particles in the considered subsystem is denoted by  $p(n)$ , and  $\rho(n)$  is the block of the reduced density matrix with  $n$  particles. Note that Eq. (1) has a beautiful structure:  $S_N$  only depends on the probability distribution of particles while  $S_{\text{conf}}$  is the von-Neumann entropy of the block  $\rho(n)$  of the reduced density matrix weighted by the probability of finding  $n$  particles in the subsystem.  $S_N$

\* zhaoyang2017@nwpu.edu.cn

† fengdingyi@nwpu.edu.cn

‡ sirker@physics.umanitoba.ca

does measure particle fluctuations while  $S_{\text{conf}}$  measures the degree of superposition between different configurations with the same particle number. Apart from being of theoretical interest, this separation of the entanglement entropy into two parts is also useful for experimental studies [12]. Since  $S_N$  is much easier to measure than the total entanglement entropy—which typically requires to resort to a full quantum tomography—it is intriguing to try to characterize  $S$  by  $S_N$  alone. For Gaussian systems—whether they are clean or disordered—it has been recently shown that this is indeed possible and that the relation  $S \sim \exp(S_N)$  holds [30].

Within the last decade, the question whether or not localization is also possible in interacting systems has received renewed attention [7, 8, 36–41]. Numerical studies of the spin-1/2 Heisenberg chain with local magnetic fields drawn from a box distribution have been interpreted in terms of an ergodic to many-body localized (MBL) phase transition at some finite disorder strength [38, 42]. One of the hallmarks of the putative MBL phase is the logarithmic growth of  $S(t)$  [4, 5] which is believed to be entirely driven by the configurational entropy while the number entropy saturates; there is no transport. Such behavior can be described by effective models of the MBL phase which consist of exponentially many conserved charges which are coupled by coupling constants which decay exponentially with distance [43, 44]. It is also possible to build phenomenological renormalization group flows for the ergodic-MBL transition but those are based on the assumption that isolating clusters do exist and that there are no resonances [45–47]. Lately, however, the stability of the MBL phase in the thermodynamic limit has been challenged in a number of publications [31, 32, 48–50]. In particular, it has been found that for the system sizes and times accessible in exact diagonalizations, the scaling relation  $S \sim \exp(S_N)$  continues to hold even for the strongly disordered spin-1/2 Heisenberg chain. This suggests that particle transport continues, albeit at a very slow rate, and that the system might ultimately always thermalize.

Because of the exponential growth of the Hilbert space with the number of particles in interacting systems, the system sizes which can be studied by exact diagonalizations are quite small and definitive statements about the thermodynamic limit are difficult to come by. In particular, it has been suggested that the observed growth of the number entropy in the MBL phase might be transient and related to being still too close to the transition point [51]. To gain further insights into the finite size scaling of  $S(t)$  and  $S_N(t)$  near a localization transition is one of our motivations to investigate the much better understood metal-insulator transition in the three-dimensional Anderson model from the entanglement angle. In addition, we believe that the results are interesting in their own right because the number entropy, in particular, is easily accessible in cold atomic gas experiments—which have already been used to study Anderson localization [52–54]—and thus can be a useful probe to test the crit-

ical properties at the transition. This is in contrast to inverse participation ratios of eigenfunctions which are commonly used in theoretical studies but are difficult to access experimentally.

The article is organized as follows: the model and methods used to calculate the various entanglement entropies are introduced in Sec. II. Our numerical results for the entanglement growth after the quench are presented in Sec. III. In the final section, we discuss our results in comparison to the ones obtained for the ergodic-MBL transition in one-dimensional interacting systems and conclude.

## II. MODEL AND METHODS

In this paper we consider free spinless fermions on a  $L \times L \times L$  square lattice with Hamiltonian

$$H = -t \sum_{\langle i,j \rangle} c_i^\dagger c_j + \sum_i D_i c_i^\dagger c_i \quad (2)$$

at half filling with open boundary conditions.  $c_i$  and  $c_i^\dagger$  are fermionic annihilation and creation operators on site  $i$ , respectively, and  $\langle \cdot, \cdot \rangle$  denotes nearest neighbors. The hopping amplitude  $t$  is site independent while the potentials  $D_i \in [-D/2, D/2]$  are randomly drawn from a box distribution. The three-dimensional Anderson model (2) has been extensively studied by many different methods [16, 55–58]. Numerical studies have shown, in particular, that the model has a mobility edge and that all eigenstates become localized for  $D_c \gtrsim 17$ . Furthermore, the localization length has been found to diverge at  $D_c$  with a critical exponent  $\nu \sim 1.5$ , and the wavefunctions at criticality show multifractal properties.

In the following, we will always prepare the system in the initial charge density wave (CDW) state

$$|\Psi(0)\rangle = \prod_{i_1+i_2+i_3 \text{ odd}} c_{i_1, i_2, i_3}^\dagger |0\rangle, \quad (3)$$

where  $|0\rangle$  denotes the vacuum state. We have checked explicitly that none of our conclusions are changed qualitatively if we use instead random product states as initial states. We then unitarily evolve the system to obtain the state  $|\Psi(t)\rangle = \exp(-iHt)|\Psi(0)\rangle$  at time  $t$ . Next, we divide the system into an inner cube of size  $\frac{L}{2} \times \frac{L}{2} \times \frac{L}{2}$  with the rest of the cube serving as environment, see Fig. 1. Tracing out the environment we obtain the reduced density matrix,  $\rho(t) = \text{tr}_{\text{Env}}|\Psi(t)\rangle\langle\Psi(t)|$ , which is the central object of our study. We are interested in the Rényi entanglement and number entropies of order  $\alpha$ ,

$$S^{(\alpha)} = \ln \text{tr}(\rho^\alpha)/(1 - \alpha), \quad (4)$$

$$S_N^{(\alpha)} = \ln \left[ \sum_n p^\alpha(n) \right] / (1 - \alpha),$$

which turn into the von-Neumann entanglement entropy  $S = -\text{tr} \rho \ln \rho$  and the number entropy  $S_N =$

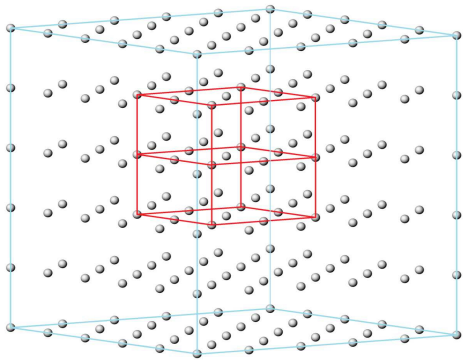


FIG. 1. A  $6 \times 6 \times 6$  cubic lattice. The considered subsystem is the  $3 \times 3 \times 3$  cube in the middle highlighted by the red frame.

$-\sum_n p(n) \ln p(n)$  in the limit  $\alpha \rightarrow 1$ . As has been shown in Ref. 30, the second Rényi entropy for Gaussian systems such as the Anderson model (2) can be bounded by the second Rényi number entropy

$$\frac{1}{e\pi} \exp\left(2S_N^{(2)}\right) - \frac{1}{6} \leq S^{(2)} \leq \frac{\ln 2}{\pi} \exp\left(2S_N^{(2)}\right). \quad (5)$$

This relation will turn out to be useful in our analysis of the numerical data.

In order to obtain the various entanglement entropies, we use the fact that for Gaussian systems the eigenvalues  $\zeta_i$  of the correlation matrix  $\mathbf{C}$  of the subsystem with matrix elements  $C_{nm} = \langle c_n^\dagger c_m \rangle$  completely determine its reduced density matrix [59–61]. In particular, the von-Neumann entanglement entropy is given by

$$S = -\sum_i (\zeta_i \ln \zeta_i + (1 - \zeta_i) \ln(1 - \zeta_i)), \quad (6)$$

and the second Rényi entropy can be obtained as

$$S^{(2)} = -\sum_i \ln(1 - 2\zeta_i(1 - \zeta_i)). \quad (7)$$

To calculate the number entropy, we need to find the probability distribution  $p(n)$ . This distribution can be obtained by evaluating the Fourier transformation of the momentum generating function  $\chi(l)$ [23, 30]:

$$p(n) = -\frac{1}{N+1} \sum_{l=0}^N \exp\left(-i \frac{2\pi l n}{N+1}\right) \chi(l), \quad (8)$$

with

$$\chi(l) = -\prod_m \left[ 1 + \left( \exp\left(\frac{i2\pi l}{N+1}\right) - 1 \right) \zeta_m \right], \quad (9)$$

and  $N = (L/2)^3$ .

Using the formulas above we are able to study the entanglement dynamics in the three-dimensional Anderson model (2) for linear system sizes of up to  $L = 22$  by exact diagonalization. We average the obtained results for the entropies over at least 200 and up to 10,000 disorder realizations.

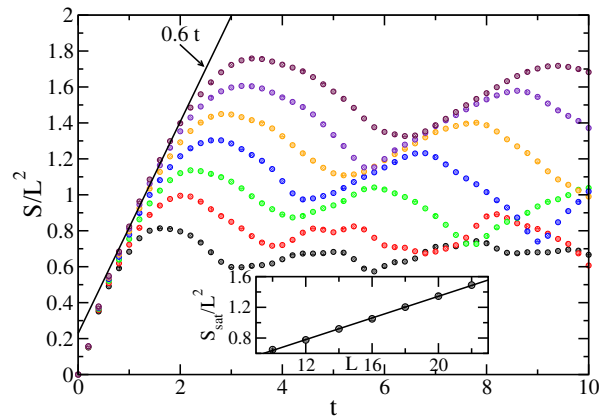


FIG. 2. Entanglement entropy  $S(t)$  for free fermions without disorder on cubic lattices with linear dimensions  $L = 10$  to  $L = 22$  (bottom to top). Inset: Averaged saturation values as function of  $L$  and a volume-law fit  $S_{\text{sat}} \sim 0.07L^3$ .

### III. RESULTS

In order to investigate the effects of the on-site disorder potential on the entanglement entropy growth following a quantum quench, we consider disorder potentials from  $D = 0$  (no disorder) up to  $D = 200$ , thus moving from the ballistic regime all the way to the strongly localized regime.

#### A. Free spinless fermions without disorder

For fermions with short-range hoppings and no disorder, we expect quite generally that a quantum quench—starting from a product state—generates quasi-particle excitations which move ballistically through the lattice with some maximum velocity  $v$  whose scale is set by the bandwidth[1]. For the chosen geometry, this will lead to a linear increase of entanglement up to times  $t \lesssim \ell/4v$  where  $\ell = L/2$  is the linear size of the subsystem. At long times, we expect an average saturation value following a volume law,  $S_{\text{sat}} \sim L^3$ . Our numerical simulations confirm this picture, see Fig. 2. We do see, in particular, that for small times all system sizes fall onto a single curve  $S(t)/L^2 \sim 0.6t$  confirming the linear increase in time. We note that the effective velocity is smaller than in the one-dimensional case [9],  $S(t) \sim 0.88t$ , but comparable to the one found for the two-dimensional square lattice [11],  $S(t)/L \sim 0.7t$ . The saturation values, around which  $S(t)$  oscillates at long times, are well fitted by a volume law, see the inset of Fig. 2.

Next, we decompose the von-Neumann entropy according to Eq. (1) into number and configurational entropy, see Fig. 3. In the thermodynamic limit we expect  $S_N \sim \nu \ln t$  with  $\nu = 1/2$  [30]. The numerical data are consistent with this expectation, see the inset of Fig. 3. The finite size corrections however are still substantial even for  $L = 22$  and the convergence to  $\nu = 1/2$  is slow.

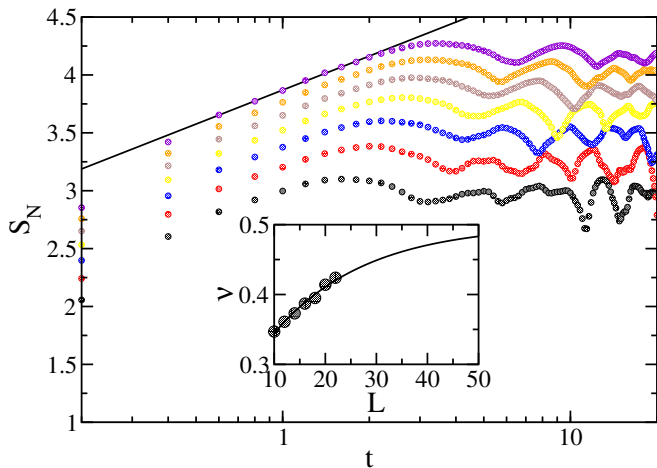


FIG. 3. Number entropy for the system without disorder for system sizes  $L = 10, 12, \dots, 22$  (from bottom to top). The line is a fit  $S_N = a + \nu \ln t$ . Inset: Fit parameters  $\nu$  as a function of system size and a fit  $\nu = 0.5 - b \exp(-\gamma L)$ .

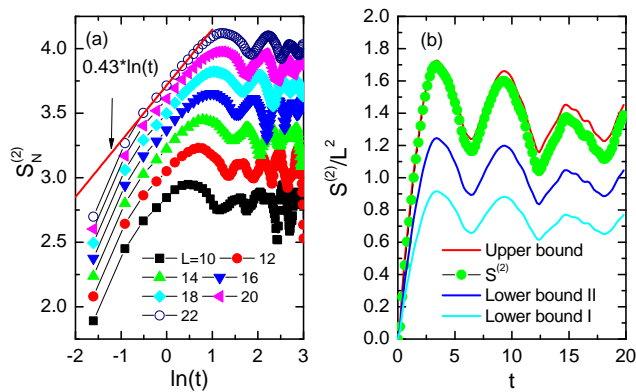


FIG. 4. (a) The second Rényi number entropy  $S_N^{(2)}$  for the system without disorder for different  $L$ . For  $L = 22$ , the scaling region is fitted by  $S_N^{(2)} \sim 0.43 \ln(t)$ . (b) The second Rényi entropy with its upper and two lower bounds,  $\exp(2S_N^{(2)})/(\epsilon\pi) - 1/6$  (Lower bound I) and  $\exp(2S_N)/(\epsilon\pi) - 1/6$  (Lower bound II).

We note that the linear growth of the total entanglement entropy is driven by the configurational entropy. The number entropy is a much smaller, sub-leading contribution.

We also consider the decomposition of the second Rényi entropy into number and configurational entropy, see Fig. 4. One can show that the scaling  $S_N^{(\alpha)} \sim \frac{1}{2} \ln t$  holds for all  $\alpha$  in a free fermionic system without disorder [30, 31]. The numerical data are in good agreement with this prediction, see Fig. 4(a), with finite-size corrections similar to  $S_N(t)$  as shown in Fig. 3. Finally, the quality of the bounds (5) is checked in Fig. 4(b). As in the one-dimensional case considered in Ref. 30, the upper bound is a fairly tight bound without disorder. More generally, it is expected that the upper bound is quite

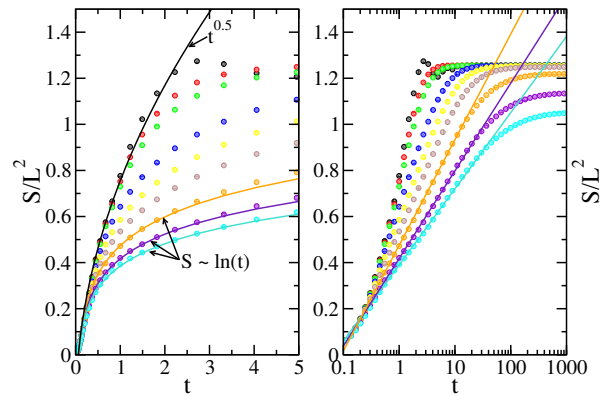


FIG. 5. The von-Neumann entropies of lattices with  $L = 16$  and  $D = 2, 4, 5, 8, 10, 12, 15, 18, 20$  (top to bottom) on a linear time scale (left panel) and a logarithmic time scale (right panel). Averages over 1000 disorder realizations are shown.

tight if the quasi-particle excitations spread ballistically while the lower bound is expected to become better in the strongly localized regime.

## B. Weak disorder and criticality

For the three-dimensional Anderson model it is known that eigenstates—depending on their energy—are starting to become localized at  $D_c \approx 16.5$ . The critical regime is characterized by a mobility edge where extended and localized eigenstates coexists and by a multifractal scaling of the inverse participation ratios of these states [57, 58]. For  $D < D_c$  we are in the metallic phase and expect diffusive behavior. For the entanglement entropy this means that we expect  $S/L^2 \sim \sqrt{t}$ . This behavior is consistent with the numerical data for  $L = 16$  and  $D \lesssim 5$ , see Fig. 5. For  $5 \lesssim D \lesssim D_c$  we see that  $S(t)$  deviates from a  $\sqrt{t}$  behavior fairly quickly due to finite-size effects. As we will show exemplarily in Fig. 7 for  $D = 16$ , the data in this regime can be fitted by an effective power law  $S(t) \sim t^\beta$  with an exponent which increases with system size and is expected to converge to  $\beta = 1/2$  in the thermodynamic limit. Physically, this is consistent with the fact that with increasing disorder fewer and fewer paths exist which allow for diffusion so that larger and larger system sizes are needed to observe it over a long time scale. It is thus clear that one has to be careful in interpreting the finite-size data: From simply fitting the data for a particular system size one might come to the conclusion that the power-law exponent in the entropy growth is decreasing below  $1/2$ . However, such sub-diffusive behavior is not expected to be present in this model and the data indeed show that the effective exponent increases towards  $1/2$  with increasing system size for all  $D < D_c$ .

For disorder strengths in the critical regime, we find that the data are well described by  $S(t) \sim \ln t$ . As shown in the right panel of Fig. 5, the data are consistent with a

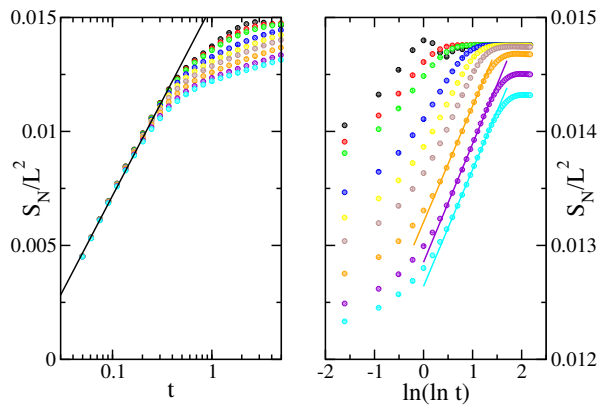


FIG. 6. The number entropies corresponding to the entanglement entropies shown in Fig. 5 on a logarithmic (left panel) and double logarithmic time scale (right panel).

logarithmic growth over almost three orders of magnitude in time. This behavior can be understood as follows: For a state at critical energy  $E_c$ , the entanglement entropy will scale as  $S/L^2 \sim \ln L$  [62]. Furthermore, we know that the localization length is given by  $\xi(E) \sim |E - E_c|^{-\nu}$  where  $\nu$  is a critical exponent with  $\nu \sim 1.5 - 1.6$  in the three-dimensional Anderson model [55, 56]. In the thermodynamic limit we might replace  $\ln L$  by  $\ln \xi(E)$ , average over energy and then replace the energy scale (bandwidth) by inverse time resulting in  $S(t)/L^2 \sim \ln t$ .

Next, we consider the number entropy  $S_N$ . According to Eq. (5), we expect a scaling  $S_N \sim \ln S$ . This behavior is confirmed by the numerical results, see Fig. 6. At short times, the number entropy for all disorder strengths increases logarithmically consistent with the initial power-law spreading of the total entanglement entropy. For disorder strengths in the critical regime, we find  $S_N \sim \ln \ln t$ , see right panel of Fig. 6. We note that the observed scaling at the metal-insulator transition in the three-dimensional Anderson model,  $S \sim \ln t$  and  $S_N \sim \ln \ln t$ , is exactly the same scaling which was recently observed in the putative many-body localized (MBL) phase of the one-dimensional Heisenberg chain [31, 32]. We will discuss possible implications for MBL physics in interacting systems further in Sec. IV.

Let us finally have a closer look at the finite-size scaling close to the critical regime on the metallic side of the transition. In Fig. 7 results for the entanglement entropy  $S(t)$  for  $D = 16$  and different system sizes are shown. We do see that the saturation value continues to increase with system size. As shown in the inset of Fig. 7 this increase is linear for the considered system sizes, showing that a volume law is fulfilled and thus implying that the system is still metallic. The time dependence is well fitted by a power law with an effective power-law exponent which, however, is an increasing function of system size and does depend on the fit interval. The logarithmic scaling observed in Fig. 5 for  $D = 16$  thus holds only approximately for  $L = 16$ . The system is still diffusive

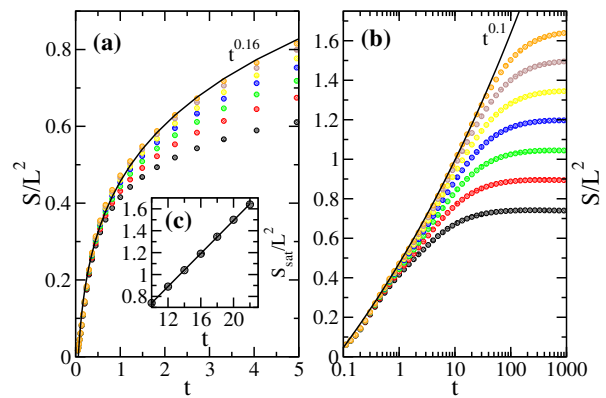


FIG. 7. Entanglement entropies for  $D = 16$  and different system sizes  $L = 10, 12, \dots, 22$  (from bottom to top) on (a) a linear, and (b) a logarithmic time scale. (c) Saturation values. 200 to 10000 samples are used for the disorder averages.

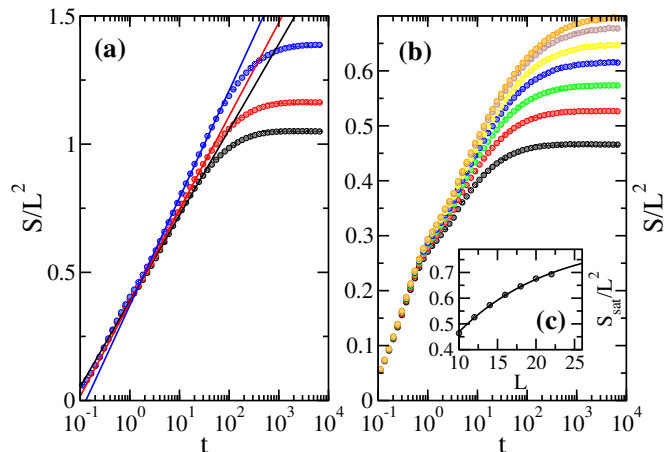


FIG. 8. (a)  $S(t)$  for  $D = 20$  and  $L = 16, 18, 22$ . The lines are logarithmic fits. (b)  $S(t)$  for  $D = 30$  and  $L = 10, 12, \dots, 22$  (bottom to top). Averages over 200 to 1,000 disorder realizations depending on system size are shown. (c) Scaling of the saturation values for  $D = 30$  as a function of  $L$  and a fit  $S_{\text{sat}}/L^2 = 0.83(1 - \exp(-0.08L))$ .

but the convergence with system size is slow and small systems already show approximately critical behavior.

When we compare this with the case  $D = 20$  shown in Fig. 8(a) we see that the data are now consistent with  $S(t) = a + \nu \ln t$  for *all system sizes* shown. Only the range of time over which the logarithmic growth is observed and the prefactor  $\nu$ —which increases slowly with increasing  $L$ —change. Note that for  $D = 20$  all eigenstates are expected to be localized, however, the localization lengths  $\xi(E)$  are much larger than the system sizes we are able to investigate so that critical behavior is observed.

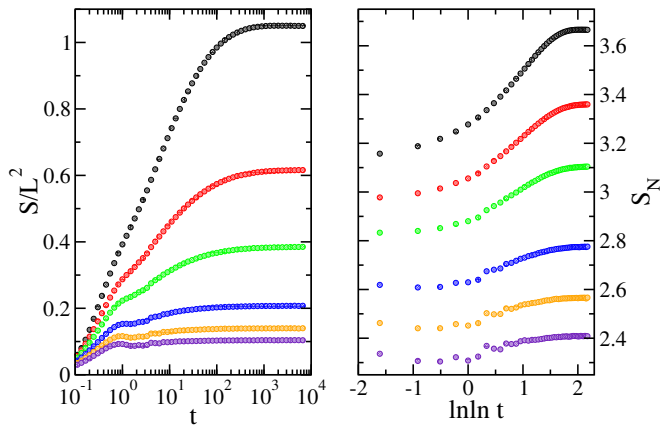


FIG. 9. Left panel:  $S(t)$  for  $D = 20, 30, 40, 60, 80, 100$  (top to bottom) with  $L = 16$  fixed. Right panel: The corresponding number entropies.

### C. Strong disorder

In the regime where all eigenstates are localized,  $D \gtrsim 17$ , both  $S(t)$  and  $S_N(t)$  will saturate in the thermodynamic limit. To observe full localization numerically, we need  $\xi \ll L$  where  $L$  are the largest system sizes considered. If this is the case, then the data will become converged in system size. As shown in Fig. 8(b), the volume law is already clearly violated for  $D = 30$  although the saturation values have not quite reached the thermodynamic limit value yet. We also note that for  $D = 30$  the growth of the entanglement entropy at intermediate times is slower than logarithmic and the scaling thus different from the critical regime.

To study the entanglement growth at intermediate times for  $D > D_c$  in more detail, we show in Fig. 9 data for different  $D$  with the size of the system kept fixed. While a logarithmic scaling is visible for  $D = 20$  at intermediate times,  $S(t)$  for large disorder strengths starts to saturate immediately after a fast initial increase and after going through a local maximum. A qualitatively similar behavior is also observed for the number entropy where an approximate  $S_N \sim \ln \ln t$  scaling at intermediate times only occurs close to the critical point while no such scaling is observed for larger disorder. This is in contrast to the putative ergodic-MBL transition in the disordered Heisenberg chain. Here the entanglement entropy continues to grow as  $S(t) \sim \ln t$  for  $D > D_c$  instead of saturating which is considered to be one of the hallmarks of MBL phases. The number entropy  $S_N(t)$ , on the other hand, should saturate if the system is truly localized. This has been called into question by recent numerical results showing that  $S_N \sim \ln \ln t$  holds even for disorders much larger than the critical value [32]. One possible explanation which has been put forward is that the observed scaling is transient and only describes the number entropy at intermediate times [51]. While the transition here is of a different kind—with both entropies

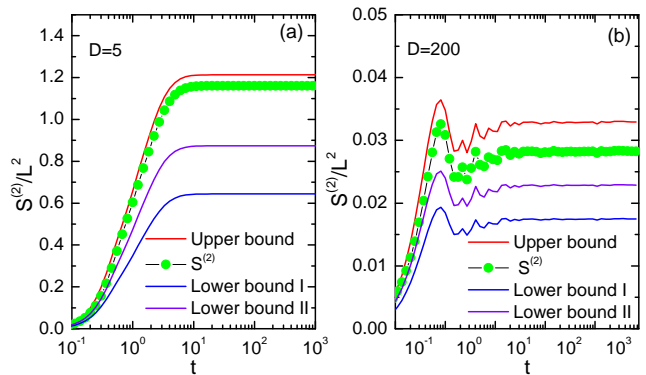


FIG. 10. The second Rényi entropy for (a)  $D = 5$  and (b)  $D = 200$  with their corresponding upper and two lower bounds,  $\exp(2S_N^{(2)})/(e\pi) - 1/6$  (Lower bound I) and  $\exp(2S_N)/(e\pi) - 1/6$  (Lower bound II).

saturation for  $D > D_c$ —it is worth noting that the saturation of  $S_N$  is observable in exact diagonalizations of systems with linear dimensions  $L \sim 20$  in contrast to the putative MBL transition where this is not the case.

To further stress the point that the saturation of both entanglement and number entropies occur at the same time scale, we show in Fig. 10 the bound (5) for the second Rényi entropy obtained from its corresponding number entropy. Both in the metallic phase and in the localized phase, the bounds show qualitatively the same time dependence as the full entropy. They do, in particular, show saturation at the same time scale. This is exactly the same behavior found for one-dimensional disordered Gaussian models in Ref. 30 and for the putative ergodic-MBL transition in the disordered Heisenberg chain in Ref. 31.

Finally, we show that our results for the entanglement entropy are consistent with what is known about the critical properties of the three-dimensional Anderson model at the metal-insulator transition. We want to stress though, that studying the entanglement growth after a quantum quench is not a suitable probe to obtain precise results for the critical properties. In particular, this probe does not offer any energy resolution. We therefore only try to show consistency with previous numerical results [16, 55–58] using the simplest scaling form where irrelevant scaling variables are completely ignored. In the localized phase, the saturation value in the thermodynamic limit is given by  $S_{\text{sat}}/L^2 \sim \xi(D)$  where  $\xi(D) \sim |D - D_c|^{-\nu}$  is the localization length which diverges at the critical disorder strength  $D_c$  with critical exponent  $\nu$ . For a finite system, we can introduce an effective length scale  $\tilde{\xi} = \xi f(L/\xi)$  with  $f(L/\xi) \rightarrow 1$  for  $L \rightarrow \infty$ . We therefore expect the following scaling collapse in the localized phase

$$\frac{S_{\text{sat}}}{\xi L^2} \propto f(L/\xi). \quad (10)$$

The two parameters controlling the scaling are: the crit-

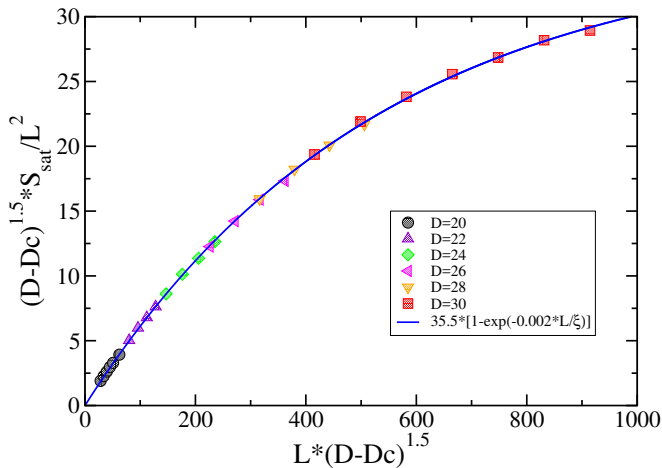


FIG. 11. Scaling collapse of the saturation values  $S_{\text{sat}}$  according to Eq. (10) for  $D_c = 18$  and  $\nu = 1.5$ .

ical disorder strength  $D_c$  and the critical exponent  $\nu$ . In Fig. 11 we show that an excellent scaling collapse can be obtained for  $D_c = 18$  and  $\nu = 1.5$ . These values are consistent with the critical disorder strength where we expect all eigenstates to become localized and with the critical exponent found in other studies [55, 56]. We note, however, that small variations of  $D_c$  and  $\nu$  are possible without drastically affecting the scaling collapse. We have not tried to fully optimize  $D_c$  and  $\nu$ ; the minimum appears to be quite shallow.

#### IV. CONCLUSIONS

We have studied the entanglement growth after a quantum quench starting from an initial product state in the three-dimensional Anderson model using exact diagonalizations. Our study has been motivated to a large extent by the recent interest in putative transitions from ergodic to many-body localized (MBL) phases in interacting models such as the Heisenberg chain with random magnetic fields. Similar to an ergodic-MBL transition, the metal-insulator transition in the 3d Anderson model is a transition where the entanglement properties change at some critical disorder. We find that in the latter case the entanglement at the critical point grows as  $S(t) \sim \ln t$  while the number entropy grows as  $S_N(t) \sim \ln \ln t$ . This is exactly the same behavior which has recently been

found for the entire numerically investigated part of the putative MBL phase in the Heisenberg chain with magnetic field disorder [31, 32]. This analogy supports the view that the MBL phase in the Heisenberg chain is not fully localized and more akin to an extended critical phase with very slow, subdiffusive particle transport. In contrast to the Heisenberg chain, we know for sure that the critical behavior in the 3d Anderson model is followed by a fully localized phase. This phase can be easily identified by exact diagonalizations using entanglement measures as a probe for linear system sizes which are similar to those considered in MBL studies of interacting systems. In particular, there is no intermediate time regime at strong disorder where  $S(t) \sim \ln t$  and  $S_N(t) \sim \ln \ln t$  still holds. Instead, for  $D \gg D_c$  an initial rapid increase is immediately followed by saturation. We have also shown that in the localized phase of the 3d Anderson model the saturation values for different disorder strengths and systems sizes can be collapsed onto a single universal scaling curve leading to values for the critical disorder strength  $D_c$  and the critical exponent  $\nu$  which are consistent with previous studies. Finally, we note that the bounds for the second Rényi entropy in terms of the corresponding number entropy give a tight upper bound for small disorder while the lower bound is approached for very strong disorder. This means that the full entanglement can be estimated quite accurately from a measurement of the number entropy alone. We believe this to be quite useful for experiments on cold atomic gases where the particle number distribution and thus the number entropy are easily accessible while a measurement of the full entanglement entropy requires quantum tomography which is currently only possible for very small system sizes.

#### ACKNOWLEDGMENTS

Y. Zhao and Dingyi Feng acknowledge support by Fundamental Research Funds for the Central Universities (3102017OQD074, 310201911cx044, 3102017OQD062, 3102017jghk02011) and National Natural Science Foundation of China (NSFC) (61705185). J. Sirker acknowledges support by the Natural Sciences and Engineering Research Council (NSERC, Canada) and by the Deutsche Forschungsgemeinschaft (DFG) via Research Unit FOR 2316.

- 
- [1] P. Calabrese and J. Cardy, Time dependence of correlation functions following a quantum quench, *Phys. Rev. Lett.* **96**, 136801 (2006).  
 [2] E. H. Lieb and D. W. Robinson, The finite group velocity of quantum spin systems, *Commun. Math. Phys.* **28**, 251 (1972).

- [3] S. Bravyi, M. B. Hastings, and F. Verstraete, Lieb-robinson bounds and the generation of correlations and topological quantum order, *Phys. Rev. Lett.* **97**, 050401 (2006).  
 [4] M. Žnidarič, T. Prosen, and P. Prelovšek, Many-body localization in the heisenberg  $xxz$  magnet in a random field, *Phys. Rev. B* **77**, 064426 (2008).

- [5] J. H. Bardarson, F. Pollmann, and J. E. Moore, Unbounded growth of entanglement in models of many-body localization, *Phys. Rev. Lett.* **109**, 017202 (2012).
- [6] P. Prelovšek, Decay of density waves in coupled one-dimensional many-body-localized systems, *Phys. Rev. B* **94**, 144204 (2016).
- [7] F. Andraschko, T. Enss, and J. Sirker, Purification and many-body localization in cold atomic gases, *Phys. Rev. Lett.* **113**, 217201 (2014).
- [8] T. Enss, F. Andraschko, and J. Sirker, Many-body localization in infinite chains, *Phys. Rev. B* **95**, 045121 (2017).
- [9] Y. Zhao, F. Andraschko, and J. Sirker, Entanglement entropy of disordered quantum chains following a global quench, *Phys. Rev. B* **93**, 205146 (2016).
- [10] Y. Zhao, S. Ahmed, and J. Sirker, Localization of fermions in coupled chains with identical disorder, *Phys. Rev. B* **95**, 235152 (2017).
- [11] Y. Zhao and J. Sirker, Logarithmic entanglement growth in two-dimensional disordered fermionic systems, *Phys. Rev. B* **100**, 014203 (2019).
- [12] A. Lukin, M. Rispoli, R. Schittko, M. E. Tai, A. M. Kaufman, S. Choi, V. Khemani, J. Leonard, and M. Greiner, Probing entanglement in a many-body-localized system, *Science* **364**, 256 (2019).
- [13] P. W. Anderson, Absence of diffusion in certain random lattices, *Phys. Rev.* **109**, 1492 (1958).
- [14] E. Abrahams, P. W. Anderson, D. C. Licciardello, and T. V. Ramakrishnan, Scaling theory of localization: Absence of quantum diffusion in two dimensions, *Phys. Rev. Lett.* **42**, 673 (1979).
- [15] J. T. Edwards and D. J. Thouless, Numerical studies of localization in disordered systems, *J. Phys. C* **5**, 807 (1972).
- [16] E. Abrahams, ed., *50 Years of Anderson Localization* (World Scientific, Singapore, 2010).
- [17] F. Iglói, Z. Szatmári, and Y.-C. Lin, Entanglement entropy dynamics of disordered quantum spin chains, *Phys. Rev. B* **85**, 094417 (2012).
- [18] T. P. Eggarter and R. Riedinger, Singular behavior of tight-binding chains with off-diagonal disorder, *Phys. Rev. B* **18**, 569 (1978).
- [19] L. Balents and M. P. A. Fisher, Delocalization transition via supersymmetry in one dimension, *Phys. Rev. B* **56**, 12970 (1997).
- [20] D. S. Fisher, Random antiferromagnetic quantum spin chains, *Phys. Rev. B* **50**, 3799 (1994).
- [21] D. S. Fisher, Random transverse field ising spin chains, *Phys. Rev. Lett.* **69**, 534 (1992).
- [22] D. S. Fisher, Critical behavior of random transverse-field ising spin chains, *Phys. Rev. B* **51**, 6411 (1995).
- [23] I. Klich and L. S. Levitov, Scaling of entanglement entropy and superselection rules, arXiv:0812.0006 (2008).
- [24] H. M. Wiseman and J. A. Vaccaro, Entanglement of indistinguishable particles shared between two parties, *Phys. Rev. Lett.* **91**, 097902 (2003).
- [25] M. R. Dowling, A. C. Doherty, and H. M. Wiseman, Entanglement of indistinguishable particles in condensed-matter physics, *Phys. Rev. A* **73**, 052323 (2006).
- [26] N. Schuch, F. Verstraete, and J. I. Cirac, Nonlocal resources in the presence of superselection rules, *Phys. Rev. Lett.* **92**, 087904 (2004).
- [27] N. Schuch, F. Verstraete, and J. I. Cirac, Quantum entanglement theory in the presence of superselection rules, *Phys. Rev. A* **70**, 042310 (2004).
- [28] H. F. Song, C. Flindt, S. Rachel, I. Klich, and K. Le Hur, Entanglement entropy from charge statistics: Exact relations for noninteracting many-body systems, *Phys. Rev. B* **83**, 161408 (2011).
- [29] H. F. Song, S. Rachel, C. Flindt, I. Klich, N. Laflorencie, and K. Le Hur, Bipartite fluctuations as a probe of many-body entanglement, *Phys. Rev. B* **85**, 035409 (2012).
- [30] M. Kiefer-Emmanouilidis, R. Unanyan, J. Sirker, and M. Fleischhauer, Bounds on the entanglement entropy by the number entropy in non-interacting fermionic systems, *SciPost Phys.* **8**, 083 (2020).
- [31] M. Kiefer-Emmanouilidis, R. Unanyan, M. Fleischhauer, and J. Sirker, Evidence for unbounded growth of the number entropy in many-body localized phases, *Phys. Rev. Lett.* **124**, 243601 (2020).
- [32] M. Kiefer-Emmanouilidis, R. Unanyan, M. Fleischhauer, and J. Sirker, Absence of true localization in many-body localized phases, arXiv:2010.00565 (2020).
- [33] R. Bonsignori, P. Ruggiero, and P. Calabrese, Symmetry resolved entanglement in free fermionic systems, *Journal of Physics A: Mathematical and Theoretical* **52**, 475302 (2019).
- [34] S. Murciano, G. D. Giulio, and P. Calabrese, Symmetry resolved entanglement in gapped integrable systems: a corner transfer matrix approach, *SciPost Phys.* **8**, 46 (2020).
- [35] S. Murciano, G. D. Giulio, and P. Calabrese, Entanglement and symmetry resolution in two dimensional free quantum field theories, *JHEP* **2020**, 73.
- [36] D. M. Basko, I. L. Aleiner, and B. L. Altshuler, Metal-insulator transition in a weakly interacting many-electron system with localized single-particle states, *Ann. Phys.* (2006).
- [37] V. Oganesyan and D. A. Huse, Localization of interacting fermions at high temperature, *Phys. Rev. B* **75**, 155111 (2007).
- [38] A. Pal and D. A. Huse, Many-body localization phase transition, *Phys. Rev. B* **82**, 174411 (2010).
- [39] D. A. Abanin, E. Altman, I. Bloch, and M. Serbyn, Colloquium: Many-body localization, thermalization, and entanglement, *Rev. Mod. Phys.* **91**, 021001 (2019).
- [40] R. Nandkishore and D. A. Huse, Many-body localization and thermalization in quantum statistical mechanics, *Annual Review of Condensed Matter Physics* **6**, 15 (2015).
- [41] E. Altman and R. Vosk, Universal dynamics and renormalization in many-body-localized systems, *Annual Review of Condensed Matter Physics* **6**, 383 (2015).
- [42] D. J. Luitz, N. Laflorencie, and F. Alet, Many-body localization edge in the random-field heisenberg chain, *Phys. Rev. B* **91**, 081103 (2015).
- [43] M. Serbyn, Z. Papić, and D. A. Abanin, Local conservation laws and the structure of the many-body localized states, *Phys. Rev. Lett.* **111**, 127201 (2013).
- [44] D. A. Huse, R. Nandkishore, and V. Oganesyan, Phenomenology of fully many-body-localized systems, *Phys. Rev. B* **90**, 174202 (2014).
- [45] R. Vosk, D. A. Huse, and E. Altman, Theory of the many-body localization transition in one-dimensional systems, *Phys. Rev. X* **5**, 031032 (2015).
- [46] A. C. Potter, R. Vasseur, and S. A. Parameswaran, Universal properties of many-body delocalization transitions, *Phys. Rev. X* **5**, 031033 (2015).
- [47] J. Z. Imbrie, Diagonalization and many-body localization for a disordered quantum spin chain, *Phys. Rev. Lett.*



- 117**, 027201 (2016).
- [48] J. Suntajs, J. Bonca, T. Prosen, and L. Vidmar, Quantum chaos challenges many-body localization, arXiv: 1905.06345 (2019).
- [49] J. Suntajs, J. Bonca, T. Prosen, and L. Vidmar, Ergodicity breaking transition in finite disordered spin chains, arXiv: 2004.01719 (2020).
- [50] D. Sels and A. Polkovnikov, Dynamical obstruction to localization in a disordered spin chain, arXiv: 2009.04501 (2020).
- [51] D. J. Luitz and Y. B. Lev, Absence of slow particle transport in the many-body localized phase, *Phys. Rev. B* **102**, 100202 (2020).
- [52] S. Ospelkaus, C. Ospelkaus, O. Wille, M. Succo, P. Ernst, K. Sengstock, and K. Bongs, Localization of bosonic atoms by fermionic impurities in a three-dimensional optical lattice, *Phys. Rev. Lett.* **96**, 180403 (2006).
- [53] G. Roati, C. D’Errico, L. Fallani, M. Fattori, C. Fort, M. Zaccanti, G. Modugno, M. Modugno, and M. Inguscio, Anderson localization of a non-interacting bose-einstein condensate, *Nature* **453**, 895 (2008).
- [54] J. Billy, V. Josse, Z. Zuo, A. Bernard, B. Hambrecht, P. Lugan, D. Clément, L. Sanchez-Palencia, P. Bouyer, and A. Aspect, Direct observation of anderson localization of matter waves in a controlled disorder, *Nature* **453**, 891 (2008).
- [55] B. R. Bulka, B. Kramer, and A. MacKinnon, Mobility edge in the three dimensional anderson model, *Z. Phys. B* **60**, 13 (1985).
- [56] K. Slevin, P. Markoš, and T. Ohtsuki, Reconciling conductance fluctuations and the scaling theory of localization, *Phys. Rev. Lett.* **86**, 3594 (2001).
- [57] L. J. Vasquez, A. Rodriguez, and R. A. Römer, Multifractal analysis of the metal-insulator transition in the three-dimensional anderson model. i. symmetry relation under typical averaging, *Phys. Rev. B* **78**, 195106 (2008).
- [58] A. Rodriguez, L. J. Vasquez, and R. A. Römer, Multifractal analysis of the metal-insulator transition in the three-dimensional anderson model. ii. symmetry relation under ensemble averaging, *Phys. Rev. B* **78**, 195107 (2008).
- [59] M.-C. Chung and I. Peschel, Density-matrix spectra of solvable fermionic systems, *Phys. Rev. B* **64**, 064412 (2001).
- [60] I. Peschel, On the reduced density matrix for a chain of free electrons, *J. Stat. Mech.*, P06004 (2004).
- [61] I. Peschel and V. Eisler, Reduced density matrices and entanglement entropy in free lattice models, *J. Phys. A* **42**, 504003 (2009).
- [62] X. Jia, A. R. Subramaniam, I. A. Gruzberg, and S. Chakravarty, Entanglement entropy and multifractality at localization transitions, *Phys. Rev. B* **77**, 014208 (2008).